The Journal of Neuroscience, August 15, 1997, 17(16):6226–6235

Differential Localization of Voltage-Dependent Calcium Channel α_1 Subunits at the Human and Rat Neuromuscular Junction

Nicola C. Day,[1] Sarah J. Wood,[2] Paul G. Ince,[1] Stephen G. Volsen,[4] William Smith,[4] Clarke R. Slater,[2] and Pamela J. Shaw[3]

[1]MRC Neurochemical Pathology Unit, Newcastle General Hospital, Newcastle upon Tyne NE4 6BE, United Kingdom, [2]Department of Neurobiology, School of Neurosciences, and [3]Division of Clinical Neurosciences, The Medical School, University of Newcastle, Newcastle upon Tyne NE2 4HH, United Kingdom, and [4]Lilly Research Centre, Windlesham, Surrey GU20 6PH, United Kingdom

Neurotransmitter release is regulated by voltage-dependent calcium channels (VDCCs) at synapses throughout the nervous system. At the neuromuscular junction (NMJ) electrophysiological and pharmacological studies have identified a major role for P- and/or Q-type VDCCs in controlling acetylcholine release from the nerve terminal. Additional studies have suggested that N-type channels may be involved in neuromuscular transmission. VDCCs consist of pore-forming α_1 and regulatory β subunits. In this report, using fluorescence immunocytochemistry, we provide evidence that immunoreactivity to α_{1A}, α_{1B}, and α_{1E} subunits is present at both rat and human adult NMJs. Using control and denervated rat preparations, we have been able to establish that the subunit thought to correspond to P/Q-type channels, α_{1A}, is localized presynaptically in discrete puncta that may represent motor nerve terminals. We also demonstrate for the first time that α_{1A} and α_{1B} (which corresponds to N-type channels) may be localized in axon-associated Schwann cells and, further, that the α_{1B} subunit may be present in perisynaptic Schwann cells. In addition, the α_{1E} subunit (which may correspond to R/T-type channels) seems to be localized postsynaptically in the muscle fiber membrane and concentrated at the NMJ. The possibility that all three VDCCs at the NMJ are potential targets for circulating autoantibodies in amyotrophic lateral sclerosis is discussed.

Key words: calcium channels; neuromuscular junction; motor neuron; Schwann cells; skeletal muscle; amyotrophic lateral sclerosis; rat; human

Voltage-dependent calcium channels (VDCCs) play a major role in neuromuscular transmission by allowing calcium ion influx into motor neuron (MN) terminals and thereby effecting acetylcholine release. VDCCs have been classified electrophysiologically into T (low-voltage-activated; LVA) and L, N, P, Q, and R (high-voltage-activated; HVA) subtypes. These channels are composed of at least three subunits: a pore-forming α_1 subunit and structural/regulatory $\alpha_2\delta$ and β subunits. Multiple α_1 gene products have been identified, termed α_{1A}, α_{1B}, α_{1C}, α_{1D}, and α_{1E} (Snutch et al., 1990; Williams et al., 1992a,b, 1994; Soong et al., 1993; Zahl et al., 1994). Although there has been debate as to whether α_{1A} is the pore-forming subunit of P and/or Q channels (Zhang et al., 1993; Stea et al., 1994), α_{1B} is thought to encode N channels (Williams et al., 1992a,b), and α_{1C} and α_{1D} are thought to be components of L channels. The identity of the channel formed after expression of α_{1E} remains unclear (Soong et al., 1993; Zhang et al., 1993; Schneider et al., 1994; Williams et al., 1994; Bourinet et al., 1996).

At the mammalian neuromuscular junction (NMJ) most evidence suggests that P and/or Q channels control acetylcholine release from MN terminals (Sano et al., 1987; De Luca et al., 1991; Uchitel et al., 1992; Protti and Uchitel, 1993; Bowersox et al., 1995; Hong and Chang, 1995; Protti et al., 1996) although there are some data suggesting that N channels also may play a role in this process (Hamilton and Smith, 1992; Hong et al., 1992; Rossoni et al., 1994). Determination of the α_1 subunit(s) localized at the mammalian NMJ should help to clarify which VDCC is involved in neuromuscular transmission. In addition, identification of the α_1 subunit at the human NMJ is of interest in amyotrophic lateral sclerosis (ALS), a disease characterized by degeneration of MNs, denervation atrophy of muscle (Campbell and Munsat, 1994), and defects in neuromuscular transmission (Denys and Norris, 1979; Maselli et al., 1993). In this disease it has been reported that a large proportion of patients has circulating autoantibodies directed against the α_1 subunit of VDCCs (Smith et al., 1992; Kimura et al., 1994). It is thought that VDCCs in MN terminals at the NMJ may represent targets for these autoantibodies and may play a role in MN degeneration in ALS (Appel et al., 1991; Smith et al., 1994; Mosier et al., 1995; Siklos et al., 1996).

To date, there is only one previous study of α_1 subunit localization at the NMJ. Ousley and Froehner (1994) demonstrated the presence of α_{1A}-like immunoreactivity (α_{1A}-ir) at the rat NMJ, although the pre- or postsynaptic nature of immunolabeling was not determined. In the present study we have used fluorescence immunocytochemistry with VDCC α_1 subunit-specific antibodies to determine the localization of α_{1A}, α_{1B}, and α_{1E} subunits at the human and rat NMJ. By comparison with markers of known distribution, the pre- or postsynaptic localization of these subunits was investigated at NMJs in control and denervated rat muscle.

Received Dec. 9, 1996; revised May 5, 1997; accepted June 4, 1997.

We are grateful to Lilly Research, the Muscular Dystrophy Group of Great Britain, and the Wellcome Trust for financial support. We thank Trevor Booth for technical assistance with confocal microscopy and Carol Young for producing the figures for this paper. We thank Dr. Louise Anderson for the gift of spectrin antibodies.

Correspondence should be addressed to Dr. Nicola Caroline Day, Pharmagene Laboratories, 2A Orchard Road, Royston, Hertfordshire SG8 5HD, UK.

 0270-6474/97/176226-•$05.00/0

MATERIALS AND METHODS

Tissues. Human gastrocnemius muscle was obtained from patients undergoing lower limb amputation. This material was taken from patients whose primary pathology was not associated with nerve or muscle. Blocks of muscle were frozen and stored in liquid nitrogen before use. Adult female Wistar rats (180–200 gm) were used in all other experiments. For denervation, animals were anesthetized (halothane 1–3%), and a 1 cm portion of the right leg sciatic nerve was cut out. The wound was closed, and the animals were allowed to recover for 7 d, after which time the rats were stunned and killed by cervical dislocation; then the soleus muscles were removed. Contralateral leg muscles were used as controls. Blocks of muscle were either frozen for cryostat sectioning or teased into bundles of fibers to examine NMJs *en face*. In the case of both human and rat muscle sections, frozen blocks of tissue were cut transversely (6 μm) on a cryostat microtome, and sections were thaw-mounted onto gelatin-coated slides. NMJ-containing regions of muscle were identified via a histochemical method for demonstrating the presence of cholinesterase (Karnovsky and Roots, 1964). Sections were air-dried (45 min) before storage at −20°C. For preparation of teased fibers, the muscle was pinned out and lightly fixed in 0.5% paraformaldehyde in 0.1 M phosphate buffer, pH 7.4, for 30 min and then teased in PBS into bundles of 3–10 fibers. The fixed, teased fibers were placed in 6-well tissue culture plates in PBS before immunocytochemistry. In addition to soleus muscle, a 1.5 cm portion of the sciatic nerve was removed from the mid-thigh region of control rat hind limb. This tissue was fixed in 4% paraformaldehyde (15 min) before freezing and storage in liquid nitrogen. Fixed, frozen blocks of sciatic nerve were cut at 5 μm. Slide-mounted sections were air-dried and stored at −20°C before use.

Antibodies. Polyclonal antibodies specific for human α_{1A}, α_{1B}, and α_{1E} VDCC subunits were produced and characterized as described previously (Volsen et al., 1995). Briefly, rabbits were immunized with fusion proteins comprising a region of the cytoplasmic loop between IIS6 and IIIS1 of α_{1A} (amino acids 1048–1208), α_{1B} (amino acids 983–1106), and α_{1E} (amino acids 958–1058), which were attached to glutathione *S*-transferase (GST). Immunoglobulin fractions were isolated from the resulting antisera, followed by removal of anti-GST antibodies and immunopurification on α_1-GST-linked Sepharose 4B columns. Residual cross-reacting antibodies were removed by further immunoadsorption. The specificity of each antisera was confirmed by immunofluorescent analysis of transfected HEK-293 cells and by ELISA (Volsen et al., 1995). For immunocytochemistry, the following antibody concentrations were used: 5.3 μg/ml α_{1A}, 3 μg/ml α_{1B}, and 1.2 μg/ml α_{1E}. Other primary antibodies (dilutions in parentheses) used in the present study include mouse anti-synaptophysin monoclonal antibody (1:100, Dako); mouse anti-neurofilament protein RT97 monoclonal antibody (1:10; a gift from Dr. B. Anderton, Institute of Psychiatry, London, UK; Wood and Anderton, 1981), which recognizes polyphosphorylated neurofilaments; rabbit anti-cow S100 polyclonal antibody (1:100, Dako), which recognizes both subunits of the Schwann cell calcium-binding protein, S100; mouse monoclonal anti-β-spectrin RBC25C4 (used for teased fibers, 1:10; a gift from Dr. L. Anderson, University of Newcastle upon Tyne, UK) (Bewick et al., 1992); and NCLSPEC2 (used for sections, 1:50; NovoCastra Laboratories, Newcastle, UK), both of which were raised to human red blood cell ghosts but recognize β-spectrin in muscle. Labeling with primary antibodies was visualized by using rhodamine-conjugated swine anti-rabbit and rabbit anti-mouse secondary antibodies (1:100, Dako, High Wycombe, UK). The secondary antibodies were preincubated with normal rat serum (ratio 2:1) for 1 hr at room temperature before application to muscle preparations. All antibody dilutions were made in PBS containing 3% BSA and 0.1 M lysine.

Immunocytochemistry. Both sections and teased fiber preparations were double-labeled with a marker for the NMJ and with antibodies to the proteins of interest. In human muscle sections, NMJs were identified by using fluorescein isothiocyanate (FITC)-conjugated dolichos biflorus lectin (DBA, 5 μg/μl, Sigma, Poole, UK), which binds to *N*-acetyl-D-galactosamine residues in the basal lamina that are concentrated at the NMJ (Sanes and Cheney, 1982). In rat muscle sections and teased fibers, NMJs were identified by labeling acetylcholine receptors with FITC-conjugated α-bungarotoxin (BgTX, 6×10^{-7} M; Molecular Probes, Eugene, OR). The NMJ markers were applied at the same time as the secondary antibodies.

All labeling procedures were performed at room temperature, and all washes were in PBS except where stated. Thawed cryostat sections were permeabilized with 0.1% Triton X-100 in PBS for 5 min. Then sections were washed for 15 min and incubated in primary antibody at 4°C overnight (~15 hr). After being washed for 1 hr, sections then were incubated in secondary antibodies, together with an NMJ marker (either FITC-DBA or FITC-BgTX), for 1 hr. After several washes over 30 min, sections were fixed in 1% paraformaldehyde for 30 min. Finally, sections were washed (30 min) and mounted in anti-fading fluorescence mountant (Vectashield, Vector Laboratories, Burlingame, CA). Some sections in each experiment were incubated without primary antibodies to control for nonspecific binding or cross-reactivity of the secondary antibodies. The labeling procedure for cryosections of sciatic nerve was the same as that used for sections of muscle. However, no NMJ marker was added to the secondary antibody before it was applied to the sciatic nerve sections.

For immunolabeling of teased muscle fiber preparations, all incubations were performed in 6-well tissue culture plates. Permeabilization of teased fibers was achieved with 1% Triton X-100 (30 min) for all antibodies, except for synaptophysin, which required permeabilization with absolute alcohol (−20°C, 10 min). After permeabilization, preparations were washed (30 min) and incubated in primary antibody at 4°C overnight. Subsequently, the fibers were washed (1 hr) before incubation with secondary antibody (plus FITC-BgTX) for 2 hr. Then preparations were washed (30 min), refixed in 1% paraformaldehyde (15 min), and placed in PBS before mounting. Teased fibers were mounted onto slides in Vectashield.

Microscopy and photography. Preparations were viewed and photographed on a Nikon Optiphot-2 microscope with a Nikon 40× oil plan apo objective. A Nikon G-2A filter set was used to photograph the rhodamine fluorescence. The FITC fluorescence was photographed through a Nikon B-2A filter set, the selectivity of which was enhanced by using a Leitz 525/20 nm bandpass emission filter to avoid "bleed through" of the rhodamine signal. The exposure times and printing conditions were the same for all photographs in each figure. In some experiments double-labeled *en face* NMJs were viewed with a confocal laser microscope (laser λ 488 nm for FITC, laser λ 568 nm for rhodamine; Bio-Rad MRC600, Munich, Germany) with a 20× [numerical aperture (NA) 0.4] and 40× (NA 0.7) objective.

RESULTS

The distribution of α_{1A}, α_{1B}, and α_{1E} subunits at the NMJ was studied in sections of human and rat muscle and in teased fibers from control and denervated rat muscle. To determine the localization of these subunits at the NMJ and to confirm denervation, we also labeled human and rat muscle preparations with marker antibodies to neurofilament, synaptophysin, S100, and β-spectrin, which are localized in preterminal axons, nerve terminals, Schwann cells, and the muscle fiber cytoskeleton, respectively.

VDCC subunit localization at the human NMJ

The distribution of VDCC α_1 subunits at the human NMJ in transverse sections of gastrocnemius muscle is shown in Figure 1. Sections were dual-labeled with DBA to identify the NMJ (*left-hand images*) and antibodies (*Ab*; *right-hand images*) directed against α_{1A} (*A*), α_{1B} (*B*), α_{1E} (*C*), neurofilament (*D*), S100 (*E*), and β-spectrin (*F*). In all sections DBA labeling was concentrated at the NMJ (intense white areas) and also was evident around the outside of the muscle fiber, consistent with the labeling of sugar residues in the basal lamina surrounding the muscle fiber membrane (Sanes and Cheney, 1982). Comparison of DBA binding with antibody labeling revealed that α_{1A}-ir (*A*) and α_{1B}-ir (*B*) were localized only at the NMJ, similar to the labeling pattern seen with neurofilament (*D*) and S100 antibodies (*E*). The α_{1E} antibody (*C*) labeled the NMJ and around the outside of the muscle fiber. This pattern of labeling is similar to that observed for the cytoskeletal muscle protein, β-spectrin (*F*) (Bewick et al., 1992), which is concentrated at the NMJ because of membrane folding. In addition, α_{1E}-ir (*C*) was observed in blood vessels lying between muscle fibers. When primary antibody was omitted from the immunostaining procedure, virtually no labeling was observed (data not shown).

The results show that α_{1A}-ir, α_{1B}-ir, and α_{1E}-ir are all localized

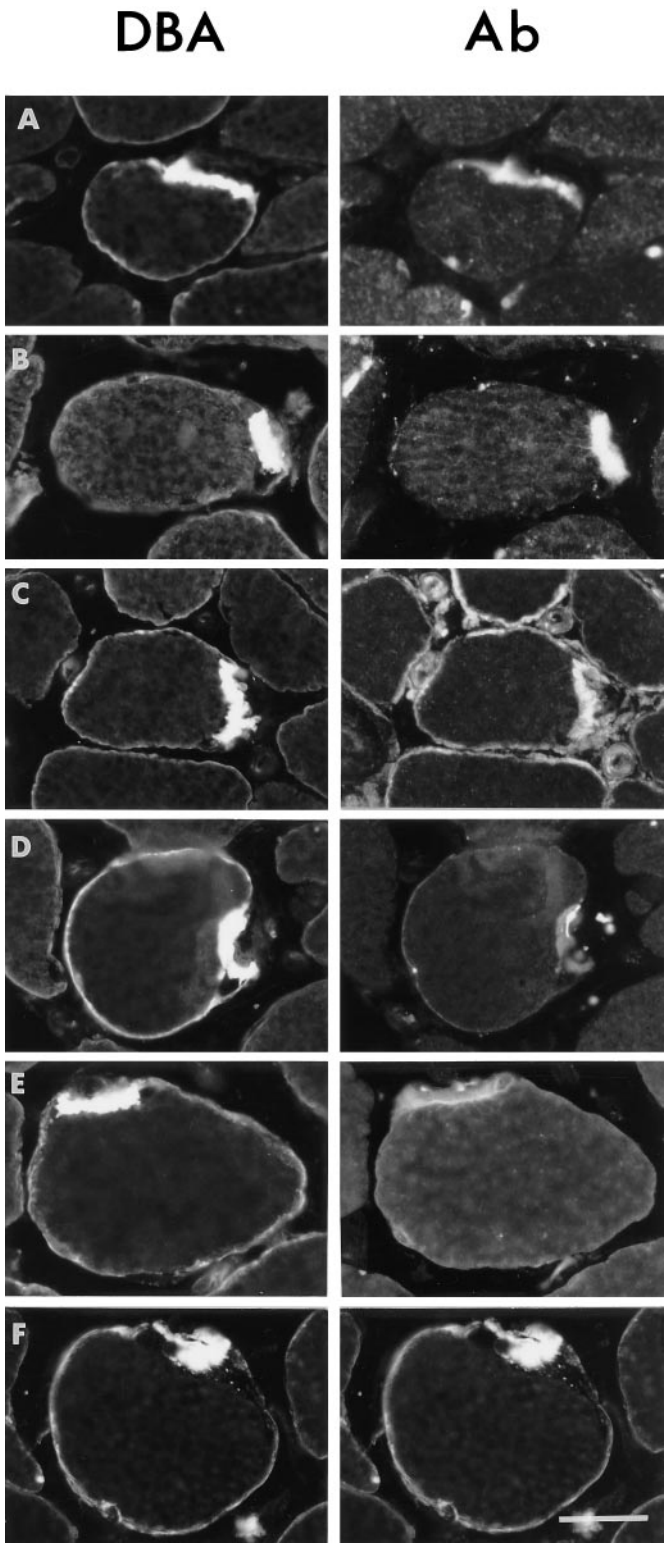

Figure 1. Distribution of α_{1A} (*A*), α_{1B} (*B*), α_{1E} (*C*), neurofilament (*D*), S100 (*E*), and β-spectrin (*F*) at the human NMJ in transverse sections of gastrocnemius muscle. Sections were dual-labeled with FITC-conjugated DBA to identify the NMJ (*left-hand images*) and primary antibodies to the above proteins, followed by rhodamine-conjugated secondary antibodies (*right-hand images*). α_{1A}-ir (*A*) and α_{1B}-ir (*B*) were localized only at the NMJ. The α_{1E} antibody (*C*) labeled the NMJ and around the outside of the muscle fiber. Scale bar, 30 μm.

at the human NMJ. To determine whether immunolabeling with these antibodies was localized in pre- or postsynaptic structures at the NMJ, we studied α_1 subunit localization in control and denervated rat muscle.

VDCC subunit localization at the rat NMJ

Control and denervated muscle sections

VDCC subunit distribution in transverse sections from control and 7 d denervated rat soleus muscle is shown in Figure 2. Sections were dual-labeled with BgTX to label postsynaptic acetylcholine receptors at the NMJ and antibodies (*Ab*) to the protein of interest. In control rat muscle sections (Fig. 2*A–F*) comparison of BgTX binding with antibody labeling revealed that α_{1A}-ir (*A*), α_{1B}-ir (*B*), and α_{1E}-ir (*C*) were localized at the NMJ, as were synaptophysin-ir (*D*), S100-ir (*E*), and β-spectrin-ir (*F*). However, some differences among the labeling patterns of the various α_1 subunits were noted. At the NMJ the α_{1A} antibody (*A*) produced a punctate pattern of labeling (marked by *arrows*). Similarly, punctate labeling of the NMJ was observed with the synaptophysin antibody (*D*), which is known to be present in MN terminals. In contrast, α_{1B}-ir (*B*) and α_{1E}-ir (*C*) were localized over the entire NMJ area demarcated by BgTX binding. In addition, α_{1E}-ir (*C*) was localized around the outside of the muscle fiber, similar to β-spectrin-ir (*F*). Thus, in both rat and human muscle sections α_{1A} and α_{1B} were localized at the NMJ only, whereas α_{1E} was localized at the NMJ and the extrajunctional muscle fiber membrane.

In denervated rat muscle sections (Fig. 2*G–L*) no labeling was observed for α_{1A} (*G*), synaptophysin (*J*), and S100 (*K*) antibodies at the NMJ, whereas α_{1B}-ir (*H*), α_{1E}-ir (*I*), and β-spectrin-ir (*L*) looked very similar to that in control sections. Disappearance of synaptophysin-ir in these sections is consistent with retraction and degeneration of MN terminals in response to denervation. Labeling with the Schwann cell marker S100 should persist after denervation, although the pattern of labeling may change because Schwann cells migrate to engulf nerve terminals and send processes beyond the boundaries of the NMJ after denervation (Reynolds and Woolf, 1992; Son et al., 1996). It is unclear why, in the present study, there is an apparent lack of this marker in denervated muscle sections (*K*). One possible explanation is that the solubility of the S100 antigen resulted in its leaching out of unfixed, denervated muscle sections during immunocytochemistry. Persistence of β-spectrin-ir in denervated muscle sections is consistent with localization of this protein in the muscle fiber membrane (Bewick et al., 1992) rather than in presynaptic structures. The finding that α_{1A}-ir disappeared after denervation, whereas α_{1B}-ir and α_{1E}-ir remained, suggests that α_{1A} is localized presynaptically, whereas α_{1B} and α_{1E} are localized in structures other than MN terminals. In addition, the similarity of α_{1E} immunolabeling to β-spectrin-ir suggests that this VDCC subunit is localized in the muscle fiber membrane.

Control and denervated teased fibers

To study VDCC subunit distribution at the NMJ in more detail, we performed immunolabeling on teased fibers from control (Fig. 3*A–G*) and denervated (Fig. 3*H–N*) rat muscle. In these preparations the NMJ could be viewed *en face*, together with preterminal processes and terminal boutons. In addition, some labeled, teased fiber preparations were examined with a confocal microscope where images of antibody labeling and BgTX binding could be superimposed to show regions of colocalization. Low-magnification (Fig. 4*A–C*) and high-magnification (Fig. 4*A′–C′*)

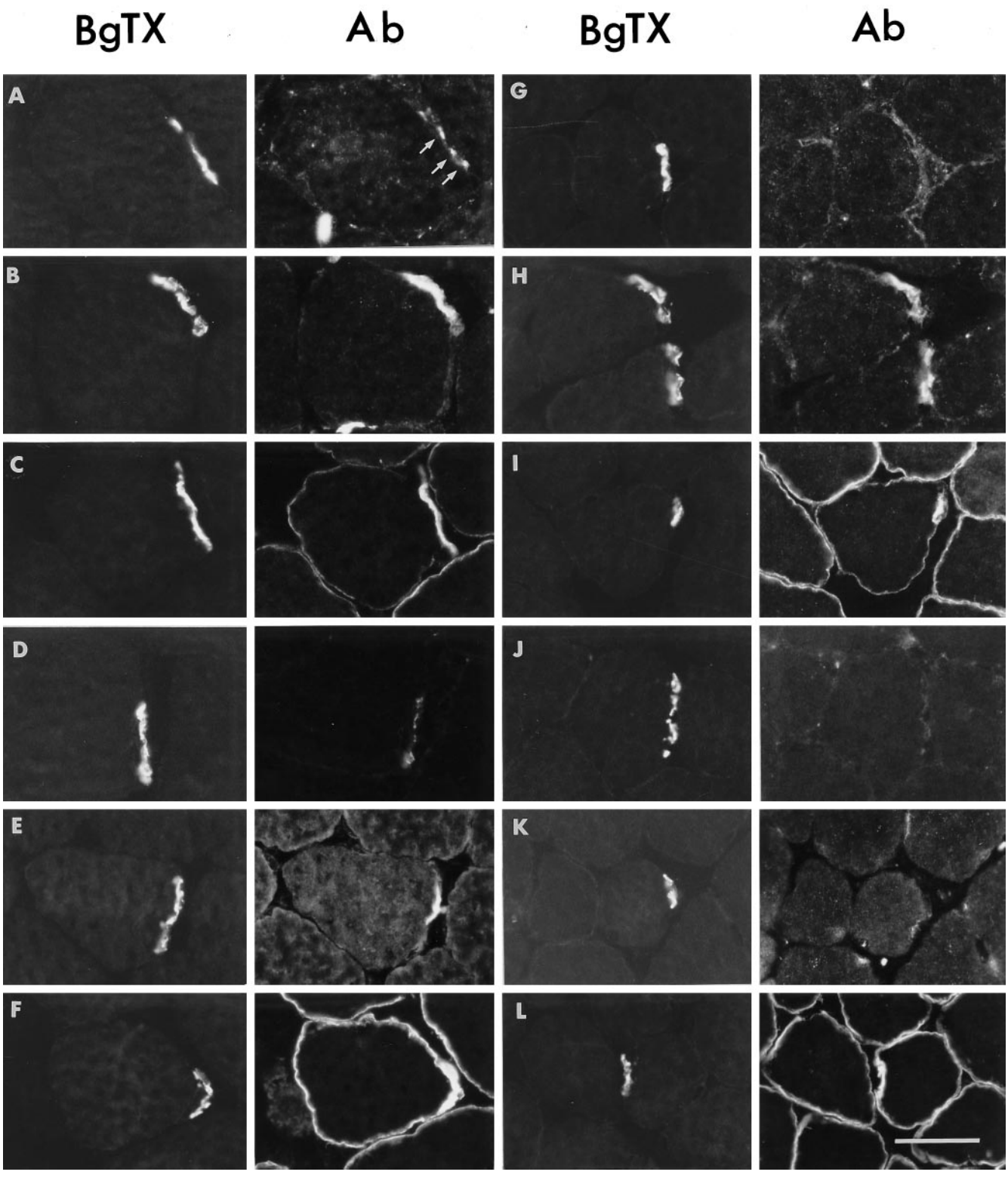

Figure 2. Distribution of α_{1A} (*A*, *G*), α_{1B} (*B*, *H*), α_{1E} (*C*, *I*), synaptophysin (*D*, *J*), S100 (*E*, *K*), and β-spectrin (*F*, *L*) at the rat NMJ in transverse sections from control (*A–F*) and denervated (*G–L*) soleus muscle. Sections were dual-labeled with BgTX to label postsynaptic acetylcholine receptors (*left-hand images*) and antibodies to the above proteins (*right-hand images*). In control sections (*A–F*) α_{1A}-ir (*A*), α_{1B}-ir (*B*), and α_{1E}-ir (*C*) were localized at the NMJ. In addition, α_{1E}-ir (*C*) was localized around the outside of the muscle fiber. In denervated sections (*G–L*) no labeling was observed with the α_{1A} antibody (*G*), whereas α_{1B}-ir (*H*) and α_{1E}-ir (*I*) looked similar to that in control sections. Scale bar, 30 μm.

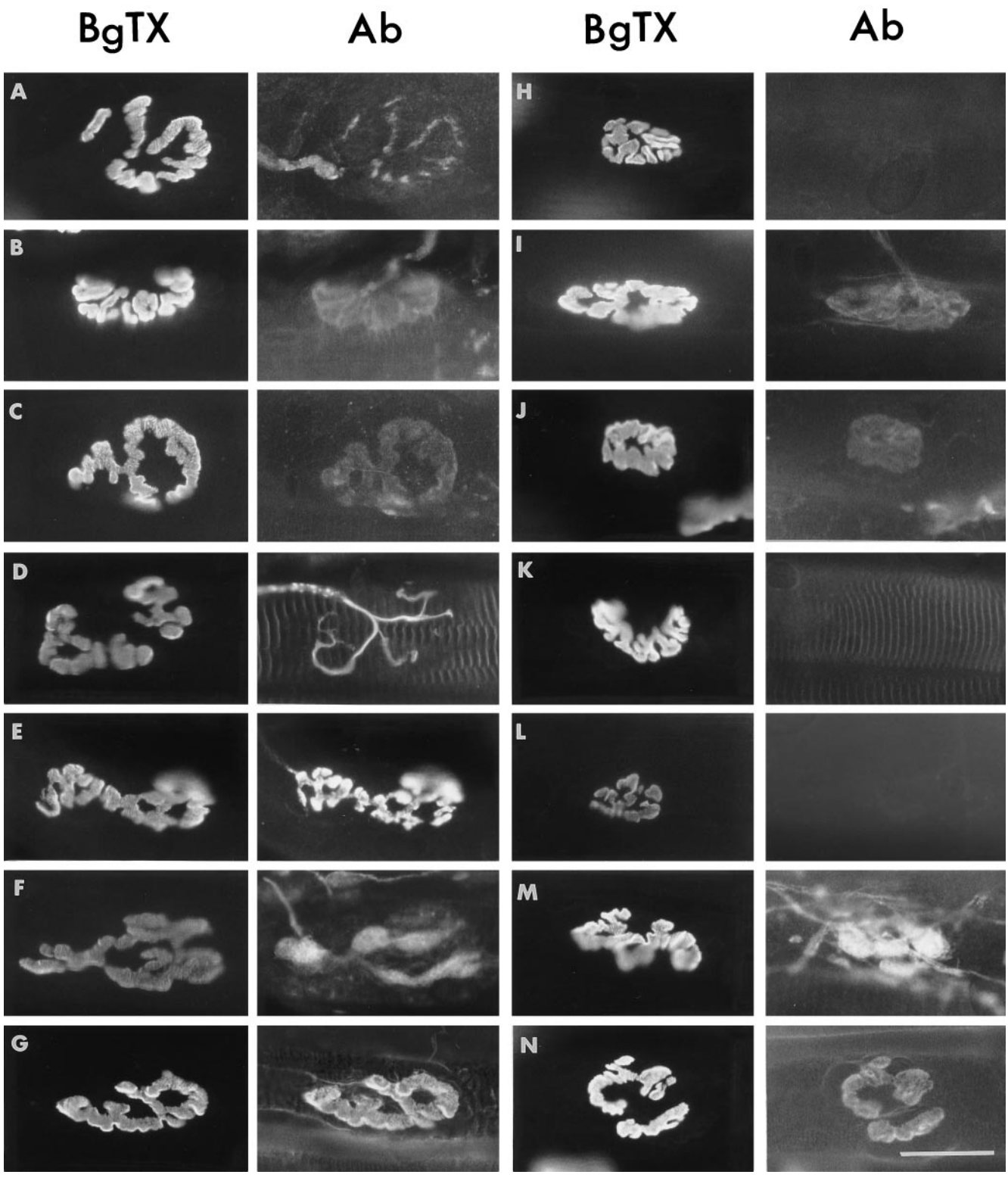

Figure 3. Distribution of α_{1A} (*A, H*), α_{1B} (*B, I*), α_{1E} (*C, J*), neurofilament (*D, K*), synaptophysin (*E, L*), S100 (*F, M*), and β-spectrin (*G, N*) at the rat NMJ in teased muscle fibers from control (*A–G*) and denervated (*H–N*) soleus muscle. Teased fibers were dual-labeled with BgTX (*left-hand images*) and the above antibodies (*right-hand images*). In control teased fibers (*A–G*), α_{1A} exhibited punctate labeling at the NMJ and also labeled processes leading into each NMJ. The α_{1B} antibody (*B*) labeled the entire surface area of the NMJ and labeled processes leading into the NMJ. Labeling with the α_{1E} antibody was concentrated at the NMJ (*C*). In denervated teased fibers (*H–N*) no labeling of the NMJ could be detected with the α_{1A} antibody (*H*). In contrast, α_{1B}-ir (*I*) and α_{1E}-ir (*J*) were similar in denervated and control teased fibers. Scale bar, 30 μm.

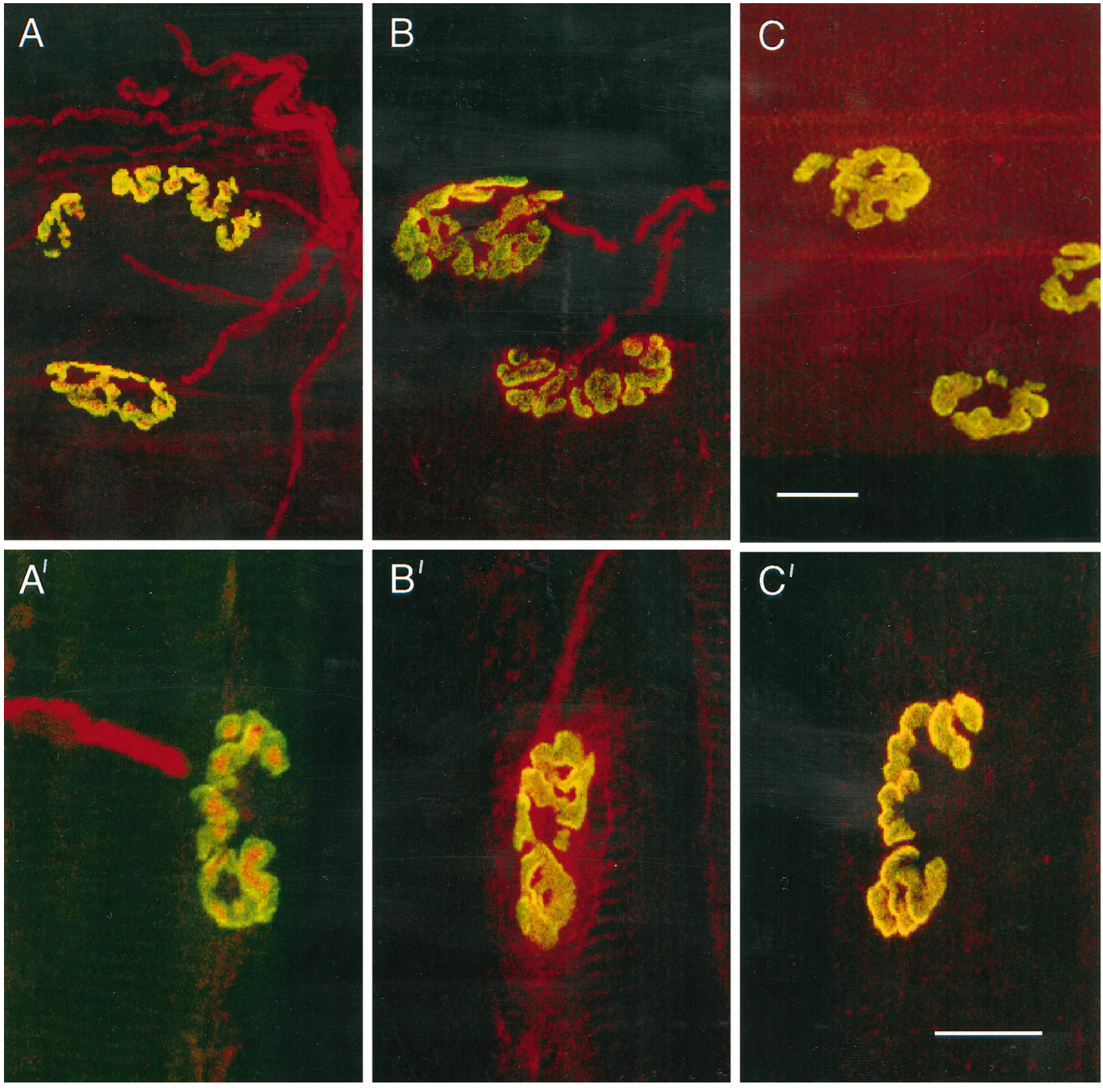

Figure 4. Pseudocolored confocal microscope images of α_{1A}-ir (*A, A′*), α_{1B}-ir (*B, B′*), and α_{1E}-ir (*C, C′*) in control rat teased muscle fibers. Preparations were dual-labeled with BgTX (*green*) and α_1 subunit antibodies (*red*). Regions of colocalization are shown in *yellow*/*orange*. Low-magnification images (20× objective) reveal that α_{1A}-ir (*A*) and α_{1B}-ir (*B*) are present in preterminal processes, whereas α_{1E}-ir (*C*) is not. Higher-magnification images (40× objective) of single NMJs show the degree of colocalization of α_1-ir with BgTX labeling. The three subunit antibodies exhibited clearly different patterns of labeling. The α_{1A} antibody (*A′*) exhibited a punctate labeling pattern that lies within the area demarcated by BgTX binding. In contrast, the α_{1B} (*B′*) antibody labeled the entire surface area of the NMJ, with labeling extending beyond the boundaries demarcated by BgTX binding, whereas α_{1E}-ir (*C′*) colocalized more precisely with BgTX binding. Scale bars: for *A–C*, 25 μm; for *A′–C′*, 20 μm.

confocal images are shown to illustrate clearly the labeling of preterminal structures and the extent of colocalization of antibody labeling and BgTX binding. In control teased fibers, comparison of BgTX binding with α_{1A}-ir (Figs. 3*A*, 4*A*,*A′*) showed that this subunit exhibited a punctate distribution over the surface of the NMJ. The extent of colocalization of α_{1A}-ir with BgTX binding is illustrated in the confocal microscope images (Fig. 4*A*,*A′*), which demonstrate that α_{1A}-labeled puncta lie within larger areas of BgTX labeling. Analysis of 11 puncta from two NMJs revealed that they were 2.7 ± 0.4 μm in length (mean ± SD), with an area of 4.7 ± 1.1 μm^2 (mean ± SD). The discrete pattern of α_{1A}-ir at the NMJ may represent localization of this subunit in clusters of active zones within individual MN terminal boutons. Labeling with the synaptophysin antibody (Fig.

3*E*) was less discrete than α_{1A}-ir and closely matched the distribution of BgTX binding. The pattern of α_{1B}-ir was quite distinct from that of both α_{1A} and α_{1E} subunits. The α_{1B} antibody labeled the entire surface area of the NMJ, with labeling extending beyond and in between the regions labeled by BgTX (Figs. 3*B*, 4*B,B′*). In contrast, α_{1E} immunolabeling of the NMJ closely matched the BgTX binding pattern (Figs. 3*C*, 4*C,C′*). Thus, the distribution of α_{1E}-ir was similar to that of the cytoskeletal muscle protein, β-spectrin (Fig. 3*G*), indicating that α_{1E} may be localized in the muscle fiber membrane. On the other hand, the distribution of α_{1B}-ir suggests that this subunit probably is not localized in the muscle fiber membrane, because a protein with this localization would match closely the distribution of BgTX binding and β-spectrin-ir.

Both α_{1A} (Figs. 3*A*, 4*A*) and α_{1B} (Figs. 3*B*, 4*B*) antibodies labeled processes leading into each NMJ. Preterminal processes also were labeled with the axonal marker, neurofilament, in addition to neurofilament-ir in sprays of terminal branches at the NMJ (Fig. 3*D*). It should be noted here that α_{1A}-labeled (Figs. 3*A*, 4*A*) and α_{1B}-labeled (Figs. 3*B*, 4*B*) preterminal processes appeared to be slightly thicker in diameter than neurofilament-labeled axons (Fig. 3*D*) and exhibited node-like structures. This labeling pattern is reminiscent of that seen with the axon-associated Schwann cell marker, myelin-associated glycoprotein (N. C. Day and S. J. Wood, unpublished observations), suggesting that α_{1A} and α_{1B} may be present in axon-associated Schwann cells (see below). The Schwann cell marker S100 was present in ovoid-shaped nuclei and processes of perisynaptic Schwann cells at the NMJ (Fig. 3*F*) and also labeled axon-associated Schwann cells.

In denervated teased fiber preparations (Fig. 3*H–N*), BgTX binding exhibited a similar distribution to that seen in control preparations, although the surface area of the NMJ was smaller because of atrophy of the muscle fiber after denervation. No labeling of the NMJ or preterminal processes could be detected with the neurofilament (Fig. 3*K*) and synaptophysin (Fig. 3*L*) antibodies, confirming that the nerve fibers and terminals had degenerated. Similarly, denervated teased fibers were devoid of α_{1A}-ir at the NMJ and in preterminal processes (Fig. 3*H*). The lack of NMJ labeling in denervated preparations further supports the notion that α_{1A}, like neurofilament and synaptophysin, is localized in presynaptic MN terminals. The lack of preterminal process labeling in denervated preparations suggests either that α_{1A} is localized in axonal processes or that this subunit is localized in axon-associated Schwann cells, which decrease α_{1A} expression in response to denervation. The data from teased fiber studies do not allow us to distinguish between these two possibilities.

In contrast to the above antibodies, α_{1B}-ir (Fig. 3*I*), α_{1E}-ir (Fig. 3*J*), S100-ir (Fig. 3*M*), and β-spectrin immunolabeling (Fig. 3*N*) persisted at the NMJ in denervated fiber preparations. These findings imply that α_{1B} and α_{1E} are localized predominantly in structures other than MN terminals or axons. Labeling with the α_{1B} antibody (Fig. 3*I*) was similar to that seen in control preparations, with α_{1B}-ir present at the NMJ and in preterminal processes. These observations, coupled with the finding that α_{1B}-ir covered a more extensive surface area than BgTX binding, suggest that α_{1B}, like S100, is not localized postsynaptically in the muscle fiber membrane but may be localized in both perisynaptic and axon-associated Schwann cells. Differences in α_{1B} and S100 labeling at the NMJ may be attributable to intense labeling of Schwann cell nuclei by the S100 antibody, but not by the α_{1B} antibody. The persistence of S100 labeling in denervated teased fiber preparations (Fig. 3*M*), compared with the lack of staining in denervated muscle sections (Fig. 2*K*, see above), could be attributable to the fact that, unlike muscle sections, teased fiber preparations were fixed before immunolabeling (possibly preventing leaching of the S100 antigen) and that the structure of the NMJ is more intact in the teased fiber preparation. The pattern of α_{1E}-ir in denervated teased fibers (Fig. 3*J*) was very similar to that in control preparations, as was β-spectrin-ir (Fig. 3*N*).

VDCC subunit localization in rat sciatic nerve

In an attempt to resolve whether α_{1A} and α_{1B} labeling of preterminal processes represented labeling of MN axons or axon-associated Schwann cells, we compared α_{1A}-ir, α_{1B}-ir, and α_{1E}-ir with S100-ir in transverse sections of rat sciatic nerve (Fig. 5). The S100 antibody produced a double-ring pattern of labeling (Fig. 5*A*), which is consistent with labeling of both inner and outer membranes of axon-associated Schwann cells. The α_{1A} (Fig. 5*B*) and α_{1B} (Fig. 5*C*) antibodies produced a similar, but fainter, pattern of labeling to S100, suggesting that both VDCC subunits are present in axon-associated Schwann cells. The complete absence of α_{1E}-ir in sciatic nerve sections (Fig. 5*D*) is consistent with other data in the present study demonstrating a lack of α_{1E}-ir in structures other than the muscle fiber membrane.

DISCUSSION

This study is the first to present a detailed comparative study on the localization of three α_1 subunits at the human and rat NMJ. We have shown that α_{1A}, α_{1B}, and α_{1E} are all found at the NMJ but seem to be localized in different cells. A comparison of control and denervated rat muscle suggests that α_{1A} is localized in MN terminals, both α_{1A} and α_{1B} may be localized in Schwann cells, and α_{1E} is localized in the muscle fiber membrane. Because the overall distribution of VDCC subunits and marker proteins in rat muscle sections is similar to that seen in human muscle sections, it seems likely that α_{1A}, α_{1B}, and α_{1E} are localized in the same cell types at the human NMJ.

VDCCs in MN terminals

Evidence that α_{1A} is localized in MN terminals comes from several observations. First, α_{1A} labeling of the rat NMJ, like the labeling observed with the presynaptic marker synaptophysin, completely disappeared after denervation. Second, the finding that α_{1A} labeling at the rat NMJ appeared as discrete puncta may be consistent with localization of α_{1A} in clusters of active zones at the presynaptic membrane of individual MN terminal boutons. Interestingly, the area of α_{1A}-labeled puncta at the rat NMJ ($4.7 \pm 1.1\ \mu m^2$; mean ± SD) compares favorably with MN terminal bouton area derived from electron microscopy ultrastructural studies in rat ($8.6\ \mu m^2$, soleus muscle; S. J. Wood, unpublished data), mouse ($3.4\ \mu m^2$, epitrochleoanconeus muscle; Lyons and Slater, 1991) and man ($2.4\ \mu m^2$, vastus lateralis; Slater et al., 1992). Although α_{1A} immunolabeling of the NMJ in rat sections was punctate in nature, this was not the case in human sections in which the α_{1A} antibody seemed to label the entire NMJ area demarcated by DBA. This could reflect localization of α_{1A} in perisynaptic Schwann cells as well as in MN terminals at the human NMJ, compared with a lack of α_{1A}-ir in rat perisynaptic Schwann cells. This observation requires further investigation, which is complicated by difficulties in obtaining suitable material.

In addition to localization at the NMJ, α_{1A} labeling was present in preterminal processes. The disappearance of α_{1A}-ir in preter-

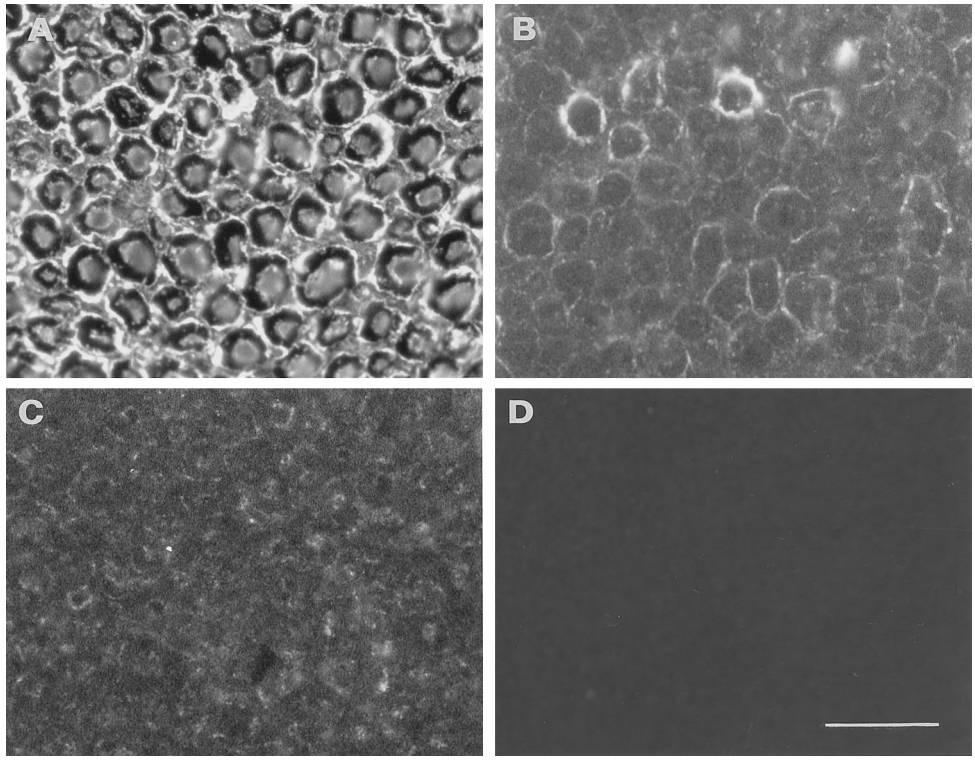

Figure 5. Distribution of S100 (*A*), α_{1A} (*B*), α_{1B} (*C*), and α_{1E} (*D*) in rat sciatic nerve sections. The S100 antibody (*A*) intensely stained a double-ring structure, consistent with labeling of the outer and inner membrane of axon-associated Schwann cells. A similar but weaker pattern of labeling was observed with α_{1A} (*B*) and α_{1B} (*C*) antibodies, whereas α_{1E}-ir (*D*) was negligible in sciatic nerve sections. Scale bar, 15 μm.

minal processes after denervation would suggest that a proportion of this subunit may be localized in MN axons. We have shown previously that MN cell bodies in human spinal cord are immunopositive for α_{1A} (Day et al., 1995). The presence of α_{1A} in MN axons would be consistent with transport of this subunit from MN cell bodies to the NMJ.

To date, there are limited anatomical data on the localization of VDCCs at the NMJ. Ousley and Froehner (1994) showed that α_{1A}-ir was present at the NMJ in transverse sections of rat muscle. However, the pre- or postsynaptic nature of α_{1A} immunolabeling was not determined in this study. Sugiura and colleagues (1995), using the Q channel ligand SNX-260, demonstrated labeling of the NMJ in teased muscle fibers from mice. A presynaptic localization for SNX-260-labeled channels was suggested by the finding that labeling was absent in denervated muscles.

Most pharmacological studies suggest that P/Q channels, but not N, L, or T channels, are involved in mammalian neuromuscular transmission. In these studies ωAga-IVA and FTX (P channel ligands; Uchitel et al., 1992; Protti and Uchitel, 1993; Bowersox et al., 1995; Hong and Chang, 1995) and ωCTX-MVIIC (Q channel ligand; Bowersox et al., 1995; Hong and Chang, 1995) blocked neuromuscular transmission, whereas ωCTX-GVIA (N channel ligand; Sano et al., 1987; De Luca et al., 1991), CGP28392 (L channel ligand; Burges and Wray, 1989), and Ni^{2+} (nonspecific T/R channel blocker; Wray and Porter, 1993; Porter and Wray, 1996) had no effect on neuromuscular transmission in mice. A similar study using human muscle showed that P, but not N or L, channels were involved in human neuromuscular transmission (Protti et al., 1996). The finding in the present study that α_{1A} is localized in MN terminals at the rat NMJ is consistent with a role for P and/or Q channels in mammalian neuromuscular transmission. A few studies have reported that ωCTX-GVIA does block rodent neuromuscular transmission (Hamilton and Smith, 1992; Rossoni et al., 1994), suggesting that N channels may play a role in this process. The results of the present study suggest that a large proportion of α_{1B} immunolabeling is localized in structures other than MN terminals. However, we cannot rule out the possibility that some α_{1B}-ir may be presynaptic, representing low-level expression of N-type channels.

VDCCs in Schwann cells

The data in the present study suggest that both α_{1A} and α_{1B} may be localized in axon-associated Schwann cells and, further, that α_{1B} also may be found in perisynaptic Schwann cells. These conclusions are based on several observations: (1) in *en face* views of NMJs in teased fiber preparations, α_{1A}-ir and α_{1B}-ir could be seen in preterminal processes; (2) both α_{1A} and α_{1B}, like S100, seemed to be localized in axon-associated Schwann cells in transverse sections of sciatic nerve; (3) in contrast to α_{1A} and α_{1E}, α_{1B} labeling in *en face* views of NMJs extended beyond and in between BgTX-labeled acetylcholine receptors on the postsynaptic membrane; and (4) like S100-ir, α_{1B} labeling of preterminal processes and the NMJ persisted in denervated teased muscle fibers. These findings are consistent with localization of α_{1A} and α_{1B} in axon-associated Schwann cells. In addition, we suggest that α_{1B} may be localized in perisynaptic Schwann cells, although the possibility that this subunit also may be localized in the muscle fiber membrane cannot be excluded. However, the contrast in labeling patterns between α_{1B} and α_{1E} antibodies indicates that if α_{1B} is localized in the muscle fiber membrane, it is restricted to the NMJ region and exhibits a distribution that is quite different from that of muscle membrane proteins such as dystrophin and β-spectrin.

Evidence for the presence of VDCCs in mammalian Schwann cells comes from a study demonstrating T- and L-type currents in cultured mouse DRG Schwann cells (Amedee et al., 1991). To date, N- and P/Q-type channels, which are thought to contain α_{1B}

and α_{1A} subunits, respectively, have not been demonstrated in mammalian Schwann cells. VDCCs in Schwann cells may be involved in Schwann cell function and Schwann cell/neuron interaction (Verkhratsky and Kettenmann, 1996). In other types of glia, activation of VDCCs has been shown to stimulate the release of neuroactive substances (Martin, 1992), regulate glial cell activity during seizure (MacVicar et al., 1991), and control myelin oligodendrocyte formation (Kirischuk et al., 1995). Although very little is known about VDCCs in synapse-associated glial cells, it is conceivable that calcium entry into perisynaptic Schwann cells via VDCCs may regulate many cellular reactions, including the release of substances that could influence neuromuscular transmission.

VDCCs in the muscle fiber

Our data suggest that α_{1E} is localized in the postsynaptic muscle fiber membrane because of its similar distribution to the cytoskeletal muscle protein, β-spectrin, and the finding that α_{1E}-ir persisted after denervation. Expression studies have produced conflicting data on the nature of the channel formed by α_{1E}. Some studies suggest that α_{1E} forms a channel that shares properties with LVA currents (Soong et al., 1993; Schneider et al., 1994; Bourinet et al., 1996), which groups it in the same category as the T channel. Other studies suggest that expressed α_{1E} resembles HVA R-type currents (Zhang et al., 1993; Schneider et al., 1994; Williams et al., 1994). Neither T nor R currents have been described in adult mammalian muscle, although the T current is expressed in immature muscle during the first 2 weeks of postnatal development (Beam and Knudson, 1988; Garcia and Beam, 1994). At present, the only VDCC described in adult muscle is the L-type channel that is involved in excitation–contraction coupling and is localized in the T-tubular network within the muscle fiber (Tanabe et al., 1988). The physiological role of α_{1E}-containing VDCCs in the muscle fiber membrane remains to be determined.

α_1 subunits at the NMJ and amyotrophic lateral sclerosis

The type of α_1 subunit at the NMJ is of interest in ALS, because it has been reported that a large proportion of patients with this disease has circulating autoantibodies directed against VDCCs (Smith et al., 1992), and these autoantibodies bind to the α_1 subunit (Kimura et al., 1994). Several lines of evidence suggest that ALS autoantibodies may interact with VDCCs in MN terminals to affect calcium flux and MN function. First, ALS IgG has been shown to increase calcium flux through P-type channels (Llinás et al., 1993) and to stimulate the spontaneous release of acetylcholine at the mouse NMJ (Appel et al., 1991). Second, mice injected with ALS IgG exhibited an increase in synaptic vesicle number and intracellular calcium levels in MN terminals (Engelhardt et al., 1995). Finally, application of ALS IgG to a differentiated hybrid MN cell line caused an increase in calcium flux (Mosier et al., 1995) and was cytotoxic to these cells (Smith et al., 1994). It has been suggested that interaction of ALS antibodies with VDCCs in MN terminals may stimulate processes leading to cell death as well as stimulating acetylcholine release (Appel et al., 1991). Interestingly, studies of muscle biopsies from ALS patients have demonstrated an increase in the probability of quantal store release (Maselli et al., 1993) and increased calcium in MN terminals (Siklos et al., 1996). The precise mechanism by which interaction of ALS autoantibodies with VDCCs at the NMJ may cause MN death is unclear, although it may involve calcium overload in MN terminals, resulting in enhanced glutamate release (Maselli et al., 1993) or altered efficacy of oxidative phosphorylation in the cell body (Siklos et al., 1996). In addition to interacting with P-type channels, ALS IgG will bind to (Smith et al., 1992) and affect calcium flux through L-type channels (Delbono et al., 1991), suggesting that VDCC autoantibodies interact with an epitope or epitopes common to several calcium channels subtypes. Thus, it seems likely that VDCCs in MN terminals, Schwann cells, and muscle will all be targets for circulating ALS autoantibodies.

In conclusion, the present study has shown that α_{1A}, α_{1B}, and α_{1E} are localized differentially at the mammalian NMJ. The major findings of our study are that α_{1A} is localized in MN terminals and that α_{1A} and α_{1B} may be present in Schwann cells, whereas α_{1E} is localized in the muscle fiber membrane. Localization of α_{1A} in MN terminals predicts that the channel incorporating this subunit may be involved in neuromuscular transmission. The role of α_{1A} and α_{1B} in Schwann cells and α_{1E} in muscle fibers is unclear, although they may play a role in regulating calcium-dependent processes within these cell types. Finally, interaction of ALS autoantibodies with α_{1A}, α_{1B}, and α_{1E} subunits at the NMJ may have important consequences for MN function and the pathogenesis of ALS.

REFERENCES

Amedee T, Ellie E, Dupouy B, Vincent JD (1991) Voltage-dependent calcium and potassium channels in Schwann cells cultured from dorsal root ganglia of the mouse. J Physiol (Lond) 441:35–56.

Appel SH, Engelhardt JI, Garcia J, Stefani E (1991) Immunoglobulins from animal models of motor neuron disease and from human amyotrophic lateral sclerosis patients passively transfer physiological abnormalities to the neuromuscular junction. Proc Natl Acad Sci USA 88:647–651.

Beam KG, Knudson CM (1988) Effect of postnatal development on calcium currents and slow charge movement in mammalian skeletal muscle. J Gen Physiol 91:799–815.

Bewick GS, Nicholson LVB, Young C, O'Donnell E, Slater CR (1992) Different distributions of dystrophin and related proteins at nerve–muscle junctions. NeuroReport 3:857–860.

Bourinet E, Zamponi GW, Stea A, Soong TW, Lewis BA, Jones LP, Yue DT, Snutch TP (1996) The α_{1E} calcium channel exhibits permeation properties similar to low-voltage-activated calcium channels. J Neurosci 16:4983–4993.

Bowersox SS, Miljanich GP, Sugiura Y, Li C, Nadasdi L, Hoffman BB, Ramachandran J, Ko CP (1995) Differential blockade of voltage-sensitive calcium channels at the mouse neuromuscular junction by novel omega-conopeptides and omega-agatoxin-IVA. J Pharmacol Exp Ther 273:248–256.

Burges J, Wray D (1989) Effect of the calcium channel agonist CGP 28392 on transmitter release at mouse neuromuscular junctions. Ann NY Acad Sci 560:297–300.

Campbell MJ, Munsat TL (1994) Motor neurone diseases. In: Disorders of voluntary muscle (Walton J, Karpati G, Hilton-Jones D, eds), pp 879–920. London: Churchill Livingstone.

Day NC, Ince PJ, Shaw PJ, Volsen SG, McCormack AL, Craig PJ, Smith W, Gillespie A, Ellis SB, Harpold MM (1995) Distribution of alpha 1A, alpha 1B, and alpha 1E voltage-dependent calcium channel subunits in the human motor system. Soc Neurosci Abstr 21:1571.

Delbono O, Garcia J, Appel SH, Stefani E (1991) Calcium current and charge movement of mammalian muscle: action of amyotrophic lateral sclerosis immunoglobulins. J Physiol (Lond) 444:723–742.

De Luca A, Rand MJ, Reid JJ, Story DF (1991) Differential sensitivities of avian and mammalian neuromuscular junctions to inhibition of cholinergic transmission by omega-conotoxin GVIA. Toxicon 29:311–320.

Denys EH, Norris FH (1979) Amyotrophic lateral sclerosis. Impairment of neuromuscular transmission. Arch Neurol 36:202–205.

Engelhardt JI, Siklos L, Komuves L, Smith RG, Appel SH (1995) Antibodies to calcium channels from ALS patients passively transferred to mice selectively increase intracellular calcium and induce ultrastructural changes in motoneurons. Synapse 20:185–199.

Garcia J, Beam KG (1994) Calcium transients associated with the T-type calcium current in myotubes. J Gen Physiol 104:1113–1128.
Hamilton BR, Smith DO (1992) Calcium currents in rat motor nerve terminals. Brain Res 584:123–131.
Hong SJ, Chang CC (1995) Inhibition of acetylcholine release from mouse motor nerve by a P-type calcium channel blocker, ω-agatoxin IVA. J Physiol (Lond) 482:283–290.
Hong SJ, Tsuji K, Chang CC (1992) Inhibition by neosurugatoxin and omega-conotoxin of acetylcholine release and muscle and neuronal nicotinic receptors in mouse neuromuscular junction. Neuroscience 48:727–735.
Karnovsky MJ, Roots L (1964) A "direct-colouring" thiocholine method for cholinesterases. J Histochem Cytochem 12:219–221.
Kimura F, Smith RG, Delbono O, Nyormoi O, Schneider T, Nastainczyk W, Hofmann F, Stefani E, Appel SH (1994) Amyotrophic lateral sclerosis patient antibodies label Ca^{2+} channel alpha 1 subunit. Ann Neurol 35:164–171.
Kirischuk S, Scherer J, Moller T, Verkhratsky A, Kettenmann H (1995) Subcellular heterogeneity of voltage-gated Ca^{2+} channels in cells of the oligodendrocyte lineage. Glia 13:1–12.
Llinás R, Sugimori M, Cherksey BD, Smith RG, Delbono O, Stefani E, Appel SH (1993) IgG from amyotrophic lateral sclerosis patients increases current through P-type calcium channels in mammalian cerebellar Purkinje cells and in isolated channel protein in lipid bilayer. Proc Natl Acad Sci USA 90:11743–11747.
Lyons PR, Slater CR (1991) Structure and function of the neuromuscular junction in young adult *mdx* mice. J Neurocytol 20:969–981.
MacVicar BA, Hochman D, Delay MJ, Weiss S (1991) Modulation of intracellular Ca^{2+} in cultured astrocytes by influx through voltage-activated Ca^{2+} channels. Glia 4:448–455.
Martin DL (1992) Synthesis and release of neuroactive substances by glial cells. Glia 5:81–94.
Maselli RA, Wollman RL, Leung C, Distad B, Palombi S, Richman DP, Salazar-Grueso EF, Roos RP (1993) Neuromuscular transmission in amyotrophic lateral sclerosis. Muscle Nerve 16:1193–1203.
Mosier D, Baldelli P, Delbono O, Smith RG, Alexianu ME, Appel SH, Stefani E (1995) Amyotrophic lateral sclerosis immunoglobulins increase Ca^{2+} currents in a motoneuron cell line. Ann Neurol 37:102–109.
Ousley AH, Froehner SC (1994) An anti-peptide antibody specific for the class A calcium channel α_1 subunit labels mammalian neuromuscular junction. Proc Natl Acad Sci USA 91:12263–12267.
Porter VA, Wray D (1996) Relative potencies of metal ions on transmitter release at mouse motor nerve terminals. Br J Pharmacol 118:27–32.
Protti DA, Uchitel OD (1993) Transmitter release and presynaptic Ca^{2+} currents blocked by the spider toxin omega-aga-iva. NeuroReport 5:333–336.
Protti DA, Reisin R, Mackinley TA, Uchitel OD (1996) Calcium channel blockers and transmitter release at the normal human neuromuscular junction. Neurology 46:1391–1396.
Reynolds ML, Woolf CJ (1992) Terminal Schwann cells elaborate extensive processes following denervation of the motor endplate. J Neurocytol 21:50–66.
Rossoni G, Berti F, La Maestra L, Clementi F (1994) Omega-conotoxin GVIA binds to and blocks rat neuromuscular junction. Neurosci Lett 176:185–188.
Sanes JR, Cheney JM (1982) Lectin binding reveals a synapse-specific carbohydrate in skeletal muscle. Nature 300:646–647.
Sano K, Enomoto KI, Maeno T (1987) Effects of synthetic ω-conotoxin, a new type Ca^{2+} antagonist on frog and mouse neuromuscular transmission. Eur J Pharmacol 141:235–241.
Schneider T, Wei X, Olcese R, Constantin JL, Neely A, Palade P, Perez-Reyes E, Qin N, Zhou J, Crawford GD, Smith RG, Appel SH, Stefani E, Birnbaumer L (1994) Molecular analysis and functional expression of the human type E neuronal Ca^{2+} channel α1 subunit. Receptors Channels 2:255–270.
Siklos L, Engelhardt J, Harati Y, Smith RG, Joo F, Appel SH (1996) Ultrastructural evidence for altered calcium in motor nerve terminals in amyotrophic lateral sclerosis. Ann Neurol 39:203–216.
Slater CR, Lyons PR, Walls TJ, Fawcett PR, Young C (1992) Structure and function of neuromuscular junctions in the *vastus lateralis* of man. A motor point biopsy study of two groups of patients. Brain 115:451–478.
Smith RG, Hamilton S, Hofmann F, Schneider T, Nastainczyk W, Birnbaumer L, Stefani E, Appel SH (1992) Serum antibodies to L-type calcium channels in patients with amyotrophic lateral sclerosis. N Engl J Med 327:1721–1728.
Smith RG, Alexianu ME, Crawford G, Nyormoi O, Stefani E, Appel SH (1994) Cytotoxicity of immunoglobulins from amyotrophic lateral sclerosis patients on a hybrid motoneuron cell line. Proc Natl Acad Sci USA 91:3393–3397.
Snutch TP, Leonard JP, Gilbert MM, Lester HA, Davidson N (1990) Rat brain expresses a heterogeneous family of calcium channels. Proc Natl Acad Sci USA 87:3391–3395.
Son YJ, Trachtenberg JT, Thompson WJ (1996) Schwann cells induce and guide sprouting and reinnervation of neuromuscular junctions. Trends Neurosci 19:280–285.
Soong TW, Stea A, Hodson CD, Dubel SJ, Vincent SR, Snutch TP (1993) Structure and functional expression of a member of the low-voltage-activated calcium channel family. Science 260:1133–1136.
Stea A, Tomlinson J, Soong TW, Bourinet E, Dubel SJ, Vincent SR, Snutch TP (1994) Localization and functional properties of a rat brain α1A calcium channel reflect similarities to neuronal Q- and P-type channels. Proc Natl Acad Sci USA 91:10576–10580.
Sugiura Y, Woppmann A, Miljanich GP, Ko CP (1995) A novel omega-conopeptide for the presynaptic localization of calcium channels at the mammalian neuromuscular junction. J Neurocytol 24:15–27.
Tanabe T, Beam KG, Powell JF, Numa S (1988) Restoration of excitation–contraction coupling and slow calcium current in dysgenic muscle by dihydropyridine receptor complementary DNA. Nature 336:134–139.
Uchitel OD, Protti DA, Sanchez V, Cherksey BD, Sugimori M, Llinás R (1992) P-type voltage-dependent calcium channel mediates presynaptic calcium influx and transmitter release in mammalian synapses. Proc Natl Acad Sci USA 89:3330–3333.
Verkhratsky A, Kettenmann H (1996) Calcium signalling in glial cells. Trends Neurosci 19:346–352.
Volsen SG, Day NC, McCormack AL, Smith W, Craig PJ, Beattie R, Ince PG, Shaw PJ, Ellis SB, Gillespie A, Harpold MM, Lodge D (1995) The expression of neuronal voltage-dependent calcium channels in human cerebellum. Mol Brain Res 34:271–282.
Williams ME, Brust PF, Feldman DH, Saraswathi P, Simerson S, Maroufi A, McCue AF, Velicelebi G, Ellis SB, Harpold MM (1992a) Structure and functional expression of an ω-conotoxin-sensitive human N-type calcium channel. Science 257:389–395.
Williams ME, Feldman DH, McCue AF, Velicelebi G, Ellis SB, Harpold MM (1992b) Structure and functional expression of α_1, α_2, and β subunits of a novel human neuronal calcium channel subtype. Neuron 8:71–84.
Williams ME, Marubio LM, Deal CR, Hans M, Brust PF, Philipson LH, Miller RJ, Johnson EC, Harpold MM, Ellis SB (1994) Structure and functional characterization of neuronal α_{1E} calcium channel subtypes. J Biol Chem 269:22347–22357.
Wood JN, Anderton BH (1981) Monoclonal antibodies to mammalian neurofilaments. Biosci Rep 1:263–268.
Wray D, Porter V (1993) Calcium channel types at the neuromuscular junction. Ann NY Acad Sci 681:356–367.
Zahl N, Simerson S, Deal C, Williams ME, Hans M, Prodanovich P, McCue AF, Sionit P, Velicelebi G, Brust PF, Johnson EC, Harpold MM, Ellis SB (1994) Cloning and functional expression of human α1A high-voltage-activated calcium channels. Soc Neurosci Abstr 20:68.
Zhang JF, Randall AD, Ellinor PT, Horne WA, Sather WA, Tanabe T, Schwarz TL, Tsien RW (1993) Distinctive pharmacology and kinetics of cloned neuronal Ca^{2+} channels and their possible counterparts in mammalian CNS neurons. Neuropharmacology 32:1075–1088.